

Electron mobility for a model $\text{Al}_x\text{Ga}_{1-x}\text{As}/\text{GaAs}$ heterojunction under pressure

X.P. Bai^{1,a} and S.L. Ban^{1,2}

¹ Department of Physics, Inner Mongolia University, Hohhot 010021, P.R. China

² CCAST (World Laboratory), P.O. Box 8730, Beijing 100080, P.R. China

Received 13 June 2006 / Received in final form 6 June 2007

Published online 28 July 2007 – © EDP Sciences, Società Italiana di Fisica, Springer-Verlag 2007

Abstract. A variational method and a memory function approach are adopted to investigate the electron mobility parallel to the interface for a model $\text{Al}_x\text{Ga}_{1-x}\text{As}/\text{GaAs}$ heterojunction and its pressure effect by considering optical phonon modes (including both of the bulk longitudinal optical (LO) in the channel side and interface optical (IO) phonons). The influence of a realistic interface heterojunction potential with a finite barrier and conduction band bending are taken into account. The properties of electron mobility versus Al concentration, electronic density and pressure are given and discussed, respectively. The results show that the electron mobility increases with Al concentration and electronic density, whereas decreases with pressure from 0 to 40 kbar obviously. The Al concentration dependent and the electron density dependent contributions to the electron mobility from the scattering of IO phonons under pressure becomes more obvious. The variation of electron mobility with the Al concentration and electron density are dominated by the properties of IO and LO phonons, respectively. The effect of IO phonon modes can not be neglected especially for higher pressure and electronic density.

PACS. 72.10.Di Scattering by phonons, magnons, and other nonlocalized excitations – 73.63.Hs Quantum wells – 63.20.Kr Phonon-electron and phonon-phonon interactions

1 Introduction

In recent decades, the optical and transport properties of electrons in quasi-two-dimensional (Q2D) systems (such as heterojunctions, quantum wells and superlattices) have been intensively studied with the fast development of microstructure science and technology. The electron-phonon interaction [1,2] has a more obvious effect on the carrier transport [3,4] and electro-optical properties [5–7] in these Q2D structures. It is possible to show qualitatively the dominant role of optical phonons influence on the electron mobility in these systems at high temperature since the detailed electron-phonon interactions were discussed [1,2,5].

In early years, Basu et al. [8] calculated the mobility of 2D excitons in an $\text{Al}_x\text{Ga}_{1-x}\text{As}/\text{GaAs}$ quantum wells (QWs) by considering various scattering processes. Hasbun [9] investigated the temperature dependence of electron mobility in a 2D heterostructures taking into account of the scattering from the LO optical phonons using a memory function approach. More recently, Anderson et al. [10] presented the relationship between electron

mobility and QW width within the Boltzmann equation approach and showed that the electron mobility increases with the well width in GaN-based QWs. The theoretical calculation of electron mobility with varying carrier density was conducted by Farvacque et al. [11]. Their results showed that the free-carrier mobility experiences a strong decrease with increasing carrier density in $\text{Al}_x\text{Ga}_{1-x}\text{N}/\text{GaN}$ QWs. However, a large part of these works adopted the 3D LO phonon approximation to estimate the electron mobility in Q2D structures without considering the detailed contribution of IO phonons, which were shown to be more important for QWs [12]. For binary compound heterojunctions, Hasbun et al. [13] discussed the electronic scattering due to different optical phonon modes and found that the combined scattering rate of the IO phonons and the half bulk optical phonons is greater than the 3D LO phonons. Pozela et al. [14] studied the relative contribution to electron mobility by confined LO and IO phonons in QWs to demonstrate the former strongly affects the electron mobility. In practice, the heterostructures consisting of ternary mixed crystals are potentially applicable. This gives an impetus to us to clarify the effect

^a e-mail: ndbaixp@imu.edu.cn

of ternary mixed crystals on the electron mobility modulated by the LO and IO phonons [7] for heterojunctions.

On the other hand, hydrostatic pressure can be used to study the physical properties in bulk and low dimensional semiconductors to provide suggestion for preparation of new materials and devices. It is well-known that pressure can shift the energy levels of tetrahedral semiconductors without altering the crystal symmetry. Up to now, there have been many works to investigate the pressure effect on the electronic effective mass, dielectric constants, and energy band, frequencies of optical phonons, etc. [15–19]. Wagner et al. [15] presented the pressure dependence of the dielectric constants and found that the dielectric constants decrease with pressure in GaN and AlN. Holtz et al. [19] conducted the optical phonon energies under pressure in $\text{Al}_x\text{Ga}_{1-x}\text{As}$ systems. The local vibrational modes in GaAs were investigated by McCluskey et al. [20]. Skierbiszewski et al. [21] studied the pressure effect on the electron mobility in GaAsN alloys and measured the pressure coefficient of the energy gap at room temperature. Their results showed that the electronic mobility decreases with pressure. However, as far as we know few works studied the pressure influence on electron mobility in such a kind of semiconductor heterojunctions, which is beneficial to understand the electronic transport properties.

In this paper, we develop a variational method and the memory function approach [13] to discuss the electron mobility in $\text{Al}_x\text{Ga}_{1-x}\text{As}/\text{GaAs}$ heterojunctions under pressure by considering both the bulk LO and IO phonons at room temperature $T = 300$ K, and also considering a realistic interface heterojunction potential model including the influences of finite potential barrier and energy band bending. Meanwhile, the tunneling of electrons into the barrier is taken into account but the scattering from the LO phonons in the barrier is neglected since it is comparatively small [7]. In our calculation, the electronic mobility versus Al concentration, electronic density and pressure are given, respectively. In Section 2, the heterojunction model and the outline of the calculation are presented; in Section 3, the pressure coefficients are discussed; Section 4 shows our calculated results and related discussions; some conclusions are finally given in Section 5.

2 Electron mobility

We consider a heterojunction consisting of two different polar semiconductors, for which the channel side GaAs denoted by material 1 is located at $z > 0$ and the barrier side $\text{Al}_x\text{Ga}_{1-x}\text{As}$ denoted by material 2 is located at $z < 0$, respectively. The interface of the heterojunction is chosen as the $x - y$ plane, which is assumed to be infinite without losing generality. To discuss the mobility of electrons in the system, we only consider the case that the electrons are confined on the lowest sub-bands of the ground states. To simplify the calculation, the optical phonon scattering is approximated to be quasi-elastic and isotropic. The variational trial wave function for an

electron can be chosen as [13]

$$\psi_k(\vec{\rho}, z) = \frac{1}{\sqrt{A}} \exp \left[i \left(\vec{k} \cdot \vec{\rho} \right) \right] \zeta(z), \quad (1)$$

with associated energy level

$$E_k = E_0 + \hbar^2 k^2 / 2m_{//}, \quad (2)$$

where the constant A is the sample area, E_0 is the electronic energy of the ground state, $\vec{k} = (k_x, k_y)$ and $\vec{\rho} = (x, y)$ are a 2D wave vector and position vector. Here the average electron band mass $m_{//}$ parallel to the $x - y$ plane is given by [13]

$$m_{//} = \frac{m_1 m_2}{(m_1 \bar{p}_2 + m_2 \bar{p}_1)}, \quad (3)$$

where \bar{p}_1 and \bar{p}_2 are the probabilities of the electron in material 1 and 2 respectively (see Ref. [13] about their detailed definitions).

In equation (1), $\zeta(z)$ describes the localization of the electrons in the z direction and satisfies [13]

$$\zeta(z) = \begin{cases} \zeta_1(z) = Db^{1/2}(bz + \beta) \exp(-bz/2) & z > 0 \\ \zeta_2(z) = D'(b')^{1/2} \exp(b'z/2) & z < 0, \end{cases} \quad (4)$$

where b and b' are the variational parameters which are obtained by minimization of the ground state energy. Constants D, D' and β depend on b and b' , their relationship are written as

$$D = \left[\beta^2 \left(1 + \frac{b}{b'} \right) + 2\beta + 2 \right]^{-1/2},$$

$$D' = \left(\frac{b}{b'} \right)^{1/2} \beta D, \quad \beta = \frac{2b}{(b + b')}.$$

The realistic heterojunction potential of the $\text{Al}_x\text{Ga}_{1-x}\text{As}/\text{GaAs}$ can be written as [13]

$$V(z) = V_0 \theta(-z) + V_s(z) + V_d(z), \quad (5)$$

where V_0 is the potential barrier height, $\theta(-z)$ is a step function. Here, $V_s(z)$ and $V_d(z)$ are the electron contribution and the depletion charge contribution to the potential, which are respectively given by

$$\frac{\partial}{\partial z} \varepsilon_0(z) \frac{\partial}{\partial z} V_s(z) = -4\pi e^2 n_s |\zeta(z)|^2$$

$$\frac{\partial}{\partial z} \varepsilon_0(z) \frac{\partial}{\partial z} V_d(z) = -4\pi e^2 [n_A(z) - n_D(z)].$$

Here, n_s is the areal electron density, $n_A(z)$ and $n_D(z)$ are the position dependent acceptor and donor concentration.

According to the Schrödinger equation in the z direction:

$$-\frac{\hbar^2}{2} \frac{\partial}{\partial z} \frac{1}{m(z)} \frac{\partial}{\partial z} \zeta(z) + V(z) \zeta(z) = E_0 \zeta(z). \quad (6)$$

One can obtain the variational energy of the ground state

$$E_0 = \langle T \rangle + \langle V_0 \rangle + \langle V_d \rangle + \langle V_s \rangle. \quad (7)$$

Then, the variational parameters can be obtained by minimizing $E_0 - \langle V_s \rangle / 2$.

The electron mobility μ in a Q2D heterojunction can be given by considering the memory function approach [13]:

$$\frac{1}{\mu} = \frac{2\hbar}{k_B T N e} \left[\sum_{\vec{q}, q_z, \lambda} |M(\vec{q}, q_z, \lambda)|^2 q_x^2 n' \left(\frac{\hbar\omega_{L\lambda}}{k_B T} \right) \prod_{02}(q, \omega_{L\lambda}) + \sum_{\vec{q}, \sigma} |M(\vec{q}, \sigma)|^2 q_x^2 n' \left(\frac{\hbar\omega_{\sigma}}{k_B T} \right) \prod_{02}(q, \omega_{\sigma}) \right]. \quad (8)$$

The first item in the right hand of equation (8) represents the electron-LO phonon interaction, and the second one is the electron-IO phonon interaction. In equation (8), \prod_{02} is the imaginary part of the 2D density-density correlation function, $n'(x)$ is the derivative of the phonon number with respect to x . Here we define $M(\vec{q}, q_z, \lambda) = M_{\lambda}(\vec{q}, q_z) I_{\lambda}(q_z)$ and $M(\vec{q}, \sigma) = A(\vec{q}, \sigma) J(q)$, where the coupling strengths $M_{\lambda}(\vec{q}, q_z)$ and $A(\vec{q}, \sigma)$ are respectively given by

$$M_{\lambda}(\vec{q}, q_z) = i \left[\frac{e^2}{\varepsilon V} \hbar\omega_{L\lambda} \left(\frac{1}{\varepsilon_{\infty\lambda}} - \frac{1}{\varepsilon_{0\lambda}} \right) \right]^{1/2} \frac{1}{Q}, \quad (9)$$

and

$$A(\vec{q}, \sigma) = i \frac{1}{\sqrt{q}} \left(\frac{\hbar e^2}{2A\omega_{\sigma}\varepsilon(\delta_{1\sigma}^2 + \delta_{2\sigma}^2)} \right)^{1/2}. \quad (10)$$

Furthermore, the matrix elements $I_{\lambda}(q_z)$ and $J(q)$ are respectively defined as

$$I_{\lambda}(q_z) = \int_{-\infty}^{\infty} |\zeta(z)|^2 \sin(q_z z) dz,$$

and

$$J(q) = \int_{-\infty}^{\infty} |\zeta(z)|^2 \exp(-q|z|) dz,$$

where $\delta_{\lambda\sigma} = \frac{(\varepsilon_{0\lambda} - \varepsilon_{\infty\lambda})^{1/2} \omega_{T\lambda}}{(\omega_{T\lambda}^2 - \omega_{\sigma}^2)}$, $\sigma = \pm$, $\lambda = 1, 2$.

ω_{σ} , the interface optical phonon frequencies, can be given by

$$\omega_{\pm}^2 = \frac{b \pm \sqrt{b^2 - 4ac}}{2a} \quad (11)$$

for high (+) and low (-) frequencies, respectively. where parameters a, b, c depend on the LO phonon frequency and transverse optical (TO) phonon frequency for material λ and relate to the Al concentration [7].

In the above equations, V is the volume of the material; the wave vector $Q = \sqrt{q^2 + q_z^2}$; $\varepsilon, \varepsilon_{\infty\lambda}$ and $\varepsilon_{0\lambda}$ are the vacuum, high frequency and static dielectric constants; $\omega_{L\lambda}$ and $\omega_{T\lambda}$ are the LO phonon frequency and transverse optical (TO) phonon frequency for material λ .

3 Pressure effect on the electron mobility

To obtain the pressure effect on the mobility of electrons in a $\text{Al}_x\text{Ga}_{1-x}\text{As}/\text{GaAs}$ heterojunction, one needs to discuss the dependence of the electronic effective mass, dielectric constants, phonon frequencies and energy band offset between GaAs and $\text{Al}_x\text{Ga}_{1-x}\text{As}$ on the hydrostatic pressure. Here pressure is confined within the range from 0 to 40 kbar [16,22] and Al concentration is in the range from 0.2 to 0.4 [23]. Thus $\text{Al}_x\text{Ga}_{1-x}\text{As}$ can be treated as a direct band gap semiconductor. The pressure-dependent electronic effective mass is given by [24]

$$\frac{m_0}{m(p)} = 1 + \frac{C}{E_g(p)}, \quad (12)$$

where $E_g(p) = E_g(0) + \alpha p$ is the band gap under pressure, $\alpha = dE_g/dp$ is the pressure coefficient of band gap and C is a constant obtained by solving equation (12) for $p = 0$.

For the pressure dependence of high frequency dielectric constant, we adopt the formula given by Goni et al. [25]

$$\frac{\partial \ln \varepsilon_{\infty}(p)}{\partial \ln V} \approx \frac{5[\varepsilon_{\infty}(p) - 1]}{3\varepsilon_{\infty}(p)} (0.9 - f_i), \quad (13)$$

where f_i is the ionicity of the material under pressure. Material volume V satisfies approximately the following linear relation in the chosen pressure range

$$B(p) = -V \frac{\partial p}{\partial V} = B_0 + B'_0 p. \quad (14)$$

Here B is the bulk modulus and may be assumed as linear with pressure for not very high pressures. B_0 and B'_0 are the bulk modulus and its first order pressure deviation at zero pressure, respectively. According to equations (13) and (14), one can write the pressure coefficient for the high frequency dielectric constant as

$$\varepsilon_{\infty}(p) = 1 + [\varepsilon_{\infty}(0) - 1] \exp\left(-\frac{5}{3B} (0.9 - f_i) p\right). \quad (15)$$

Then, the static dielectric constant is determined by the LST relation:

$$\varepsilon_0(p) = \varepsilon_{\infty}(p) \left[\frac{\hbar\omega_{LO}}{\hbar\omega_{TO}} \right]^2, \quad (16)$$

where $\hbar\omega_{LO}$ and $\hbar\omega_{TO}$ are the LO and TO phonon energies, respectively.

According to the mode-Grüneisen parameter [19]

$$\gamma = \frac{B_0}{\omega_0} \frac{\partial \omega}{\partial p}. \quad (17)$$

The dependence of optical phonon energies on pressure can be determined. In equation (17), ω_0 and ω are the optical phonon frequencies under hydrostatic pressure $p = 0$ and $p \neq 0$, respectively. Here an effective phonons mode approximation is used to consider the pressure effect [18,23].

Table 1. Parameters used in the computation (see the text about the adopted units).

	ε_0	ε_∞	$\hbar\omega_{LO}$	$\hbar\omega_{TO}$	m	f_i	B_0	B'_0	E_g	α	γ_{LO}	γ_{TO}
GaAs ^a	13.18	10.89	36.25	33.29	0.067	0.310	748 ^b	4.6 ^b	1424	11.5	1.01 ^c	1.12 ^c
AlAs ^a	10.06	8.16	50.09	44.88	0.15	0.274	770 ^b	4.6 ^b	3018	10.2	0.85 ^c	1.08 ^c

^aAdachi, reference [23]; ^bLam, reference [26]; ^cHoltz, reference [19].

The values of parameters used in our calculation are given in Table 1, where phonon energies and energy band gap are measured in units of meV, electronic effective mass in units of the bare electronic mass m_0 , bulk modulus B_0 in units of kbar and pressure coefficient of band gap α in units of meV/kbar.

4 Results and discussion

In numerical calculation of the electron mobility in an $\text{Al}_x\text{Ga}_{1-x}\text{As}/\text{GaAs}$ heterojunction under pressure, we adopt the 60:40 rule and write the barrier height as [7, 18]

$$V_0 = 0.6 \times (E_{g2} - E_{g1}), \quad (18)$$

where $E_{g2} = 1.424 + 1.247x$ for the direct band gap barrier $\text{Al}_x\text{Ga}_{1-x}\text{As}$ within $0.2 \leq x \leq 0.4$ [23]. The calculated results are shown in Figures 1–4 at room temperature $T = 300$ K.

In Figure 1, the contribution to the electron mobility from the scattering of the IO, LO and the total (IO+LO) phonons are plotted as functions of Al concentration x for given electronic density $n_s = 4.0 \times 10^{11}/\text{cm}^2$, corresponding to different pressures, respectively. Comparing Figures 1a, 1b and 1c, it is found that the electron mobility decreases as pressure increases and the scattering from the IO phonons is more sensitive to pressure. The contribution from the IO phonons becomes more and more obvious especially for small x as increasing pressure even the contribution from the LO phonons plays a more important role to decide the mobility. For examples, the ratios to the mobility from the LO phonons are 0.671, 0 kbar, 0.655, 40 kbar for $x = 0.2$, and 0.779, 0 kbar, 0.770, 40 kbar for $x = 0.4$, respectively. The two contributions are comparable so as to the IO phonons are not negligible especially under pressure. Meanwhile, one can see that the total mobility increases with x slightly at the same pressure. This is due to the competition between the contributions from the IO and LO phonons. With increasing x , the potential barrier is sensitive to pressure to enforce the electron move away from the interface into the channel side, results in the increasing of the average distance between the electron and the interface $\langle z \rangle = -D'^2/b' + D^2(6 + 4\beta + \beta^2)/b$. Thus, the scattering from the IO phonons becomes weaker and the scattering from the LO phonons becomes stronger. On the other hand, the contribution from the LO phonons is not sensitive to the change of x since the channel material is binary compound. The scattering from LO phonons increases with pressure causes the decrease of mobility. However, the net increase of mobility from the IO phonons go

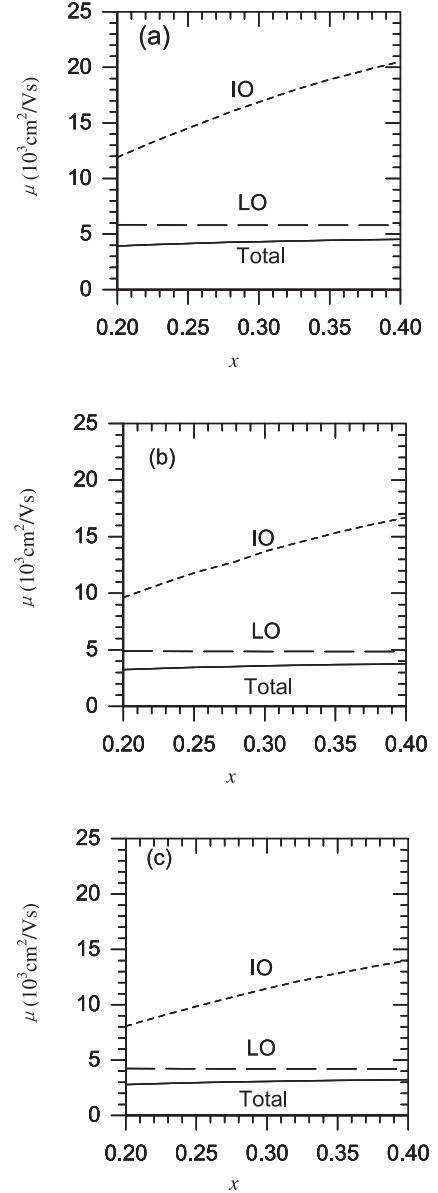


Fig. 1. Electron mobility as a function of Al concentration due to the scattering from IO (short-dashed line) and LO (long-dashed line) phonons for given electronic density $n_s = 4.0 \times 10^{11}/\text{cm}^2$, temperature $T = 300$ K, and pressures $p = 0$ kbar (a), $p = 20$ kbar (b) and $p = 40$ kbar (c), respectively. The total mobility from IO+LO scattering is denoted by the solid line and described by $\mu_T^{-1} = \mu_{IO}^{-1} + \mu_{LO}^{-1}$.

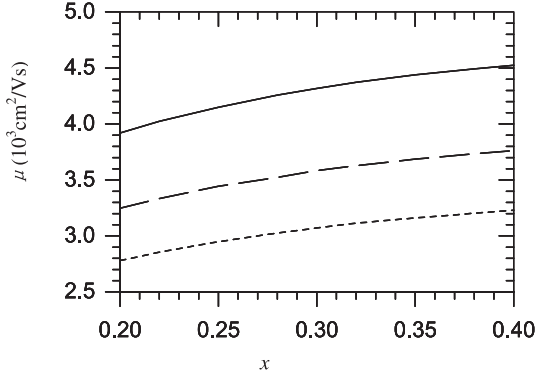


Fig. 2. Electron mobility as a function of Al concentration x for given electronic density $n_s = 4.0 \times 10^{11}/\text{cm}^2$, temperature $T = 300$ K, and pressure $p = 0, 20, 40$ kbar, corresponding to solid, long-dashed, short-dashed lines, respectively.

beyond the net decrease of mobility from the LO phonons. As a result, the electron mobility from the total phonon (IO+LO) scattering increases with x , which is mainly decided by the IO phonons.

Figure 2 shows the total electron mobility as a function of Al concentration x for given electronic density $n_s = 4.0 \times 10^{11}/\text{cm}^2$, corresponding to the different pressures $p = 0, 20$ and 40 kbar. This indicates obviously that the electronic mobility decreases with increasing pressure and the curves of mobility under pressure are similar to that at zero pressure. Comparing the results at 20 kbar and 40 kbar with that at 0 kbar, one can see that the net decreases of the mobility are 17% and 29% respectively. The electronic effective mass and phonon energies increase with pressure, but the dielectric constants and potential barrier decrease with pressure. These factors combine together to influence the energy band bending, the heterojunction potential and the intrinsic properties of the materials. The pressure-induced reduction of mobility results from the complex effects of the pressure on the electronic effective mass, dielectric constants of materials, phonon energies and potential barrier.

Figure 3 presents the contribution to the electron mobility from the scattering of the IO, LO and the total (IO+LO) phonons as a function of electronic density with $x = 0.3$, corresponding to different pressures, respectively. It is obvious that the total electron mobility increases with electronic density n_s . The reason can also be attributed to the competition between the contributions from the scattering of IO phonons and the LO phonons. As the increase of electronic density, the band bending becomes more noticeable and makes the electron move towards the interface and penetrates into the barrier side, which leads to the fact that the average distance between the electron and the interface $\langle z \rangle$ is closer to the interface. So the scattering from the IO phonons becomes stronger and the scattering from the LO phonons becomes comparatively weaker even the latter plays an important role. But the net decrease of mobility from the IO phonons are lower than the net increase of mobility from the LO phonons. As a result, the electronic mobility influenced by the scat-

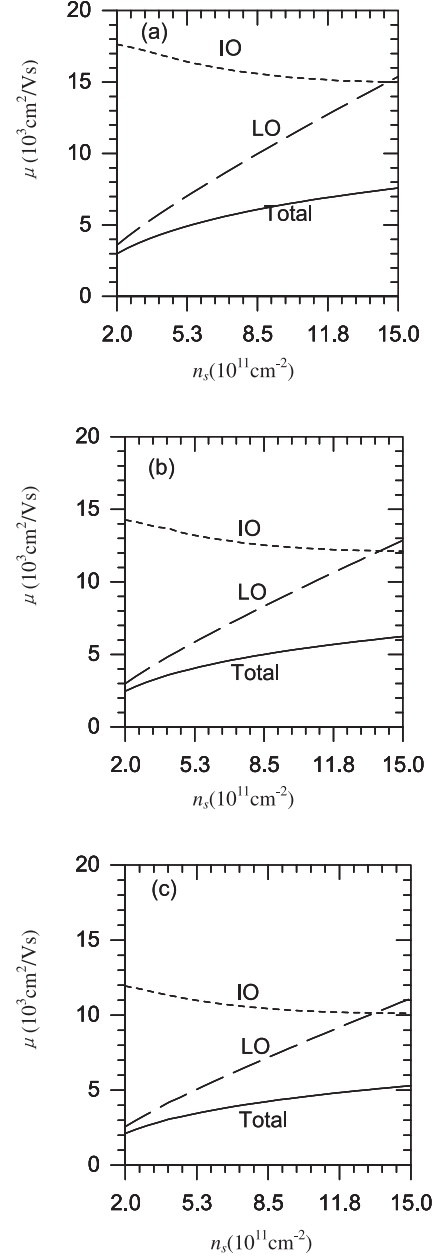


Fig. 3. Electron mobility as a function of electronic density n_s due to the scattering from IO (short-dashed line) and LO (long-dashed line) phonons for given Al concentration $x = 0.3$, temperature $T = 300$ K, and pressures $p = 0$ kbar (a), $p = 20$ kbar (b) and $p = 40$ kbar (c), respectively. The total mobility from the IO+LO scattering is denoted by the solid lines and described by $\mu_T^{-1} = \mu_{IO}^{-1} + \mu_{LO}^{-1}$.

tering of total (IO+LO) phonons increases with the electronic density. This property is decided mainly by the LO phonons, whereas the IO phonons become more and more important as increasing pressure.

Finally, in Figure 4, the total electron mobility μ versus electronic density n_s for given Al concentration $x = 0.3$ is shown corresponding to the different pressures. Here, the pressure-induced trend of mobility is similar to that in Figure 2.

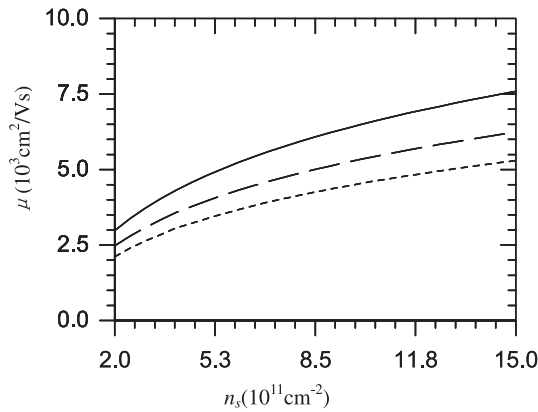


Fig. 4. Electron mobility as a function of electronic density n_s for given Al concentration $x = 0.3$, temperature $T = 300$ K, and pressure $p = 0, 20, 40$ kbar, corresponding to solid, long-dashed, short-dashed lines, respectively.

5 Conclusions

We studied the pressure effect on the electron mobility in $\text{Al}_x\text{Ga}_{1-x}\text{As}/\text{GaAs}$ with a realistic heterojunction potential by considering the scattering from the IO and LO phonons at room temperature. The results show that the electron mobility increases nonlinearly with the Al concentration and electronic density, whereas decreases with pressure from 0 to 40 kbar. The contribution to the electronic mobility from IO phonons scattering under pressure becomes more obvious. The electron mobility from the optical phonon scattering increases slightly with the Al concentration and its property is dominated by the IO phonons. The mobility increases with the electron density and is dominated by the LO phonons.

This work was supported by the National Natural Science Foundation of China (Project 60566002) and by the project for excellence subject-directors of Inner Mongolia Autonomous Region of China.

References

1. L. Wendler, Phys. Stat. Sol. B **141**, 129 (1987)
2. N. Mori, T. Ando, Phys. Rev. B **40**, 6175 (1989)
3. X.L. Lei, N.J.M. Horing, J.Q. Zhang, Phys. Rev. B **34**, 1139 (1986)
4. X.L. Lei, J.Q. Zhang, J.L. Birman, C.S. Ting, Phys. Rev. B **33**, 4382 (1986)
5. G.Q. Hai, F.M. Peeters, J.T. Devreese, Phys. Rev. B **48**, 4666 (1993)
6. S.L. Ban, X.X. Liang, R.S. Zheng, Phys. Lett. A **192**, 110 (1994)
7. S.L. Ban, J.E. Hasbun, Phys. Rev. B **59**, 2276 (1999)
8. P.K. Basu, Partha Ray, Phys. Rev. B **44**, 1844 (1991)
9. J.E. Hasbun, Phys. Rev. B **52**, 11989 (1995)
10. D.R. Anderson et al., Phys. Rev. B **63**, 245313 (2001)
11. J.-L. Farvacque, Z. Bougrioua, Phys. Rev. B **68**, 035335 (2003)
12. X.F. Wang, I.C. da Cunha Lima, X.L. Lei, Phys. Rev. B **58**, 12609 (1998)
13. J.E. Hasbun, S.L. Ban, Phys. Rev. B **58**, 2102 (1998)
14. J. Pozela et al., Physica E **5**, 108 (1999)
15. J.-M. Wagner, F. Bechstedt, Phys. Rev. B **62**, 4526 (2000)
16. B. Sukumar, K. Navaneethakrishnan, Solid State Commun. **76**, 561 (1990)
17. P. Lefebvre, B. Gil, H. Mathieu, Phys. Rev. B **35**, 5630 (1987)
18. G.J. Zhao, X.X. Liang, S.L. Ban, Phys. Lett. A **319**, 191 (2003)
19. M. Holtz et al., Phys. Rev. B **54**, 8714 (1996)
20. M.D. McCluskey et al., Phys. Rev. B **56**, 6404 (1997)
21. C. Skierbiszewski et al., Phys. Stat. Sol. B **216**, 135 (1999)
22. A.R. Goni et al., Phys. Rev. B **36**, 1581 (1987)
23. S. Adachi, J. Appl. Phys. **58**, R1 (1985)
24. D.Z.-Y. Ting, Yia-Chung Chang, Phys. Rev. B **36**, 4359 (1987)
25. A.R. Goni, K. Syassen, M. Cardon, Phys. Rev. B **41**, 10104 (1990)
26. P.K. Lam, M.L. Cohen, G. Martinez, Phys. Rev. B **35**, 9190 (1987)